Community structure – ecosystem function relationships in the Congo Basin methane cycle depend on the physiological scale of function

Kyle M. Meyer[1#*+], Anya M. Hopple[1#], Ann M. Klein[1], Andrew H. Morris[1], Scott Bridgham[1], Brendan J. M. Bohannan[1]

1. Institute of Ecology and Evolution, University of Oregon, Eugene, OR, USA

# Authors contributed equally to the preparation of this manuscript

*Corresponding author: kmmeyer@berkeley.edu

+ Present address: Department of Integrative Biology, University of California – Berkeley, Berkeley, CA, USA

Keywords: Biodiversity-Ecosystem Function, Congo Basin, Methane, Microbial ecology

Running title: Structure – function relationships in the tropical methane cycle

ABSTRACT

Belowground ecosystem processes can be highly variable and difficult to predict using microbial community data. Here we argue that this stems from at least three issues: 1) complex covariance structure of samples (with environmental conditions or spatial proximity) can make distinguishing biotic drivers a challenge, 2) communities can control ecosystem processes through multiple mechanisms, making the identification of these controls a challenge and 3) ecosystem function assessments can be broad in physiological scale, encapsulating multiple processes with unique microbially mediated controls. We suggest that these problems can be overcome by addressing environmental variability and sample covariance structure, separating microbial community measurements into distinct attributes that represent putative controls, and resolving functions to finer physiological scales. We test these assertions using methane (CH_4)-cycling processes in soil samples collected along a wetland-to-upland habitat gradient in the Congo Basin. We perform our measurements of function under controlled laboratory conditions and include environmental covariates in statistical analyses to aid in identifying biotic drivers. We divide measurements of microbial communities into four attributes (abundance, activity, composition, and diversity) that represent different forms of community control. Lastly, our process measurements differ in physiological scale, including broader scales (gross methanogenesis and methanotrophy) that involve more mediating groups, to finer scales (hydrogenotrophic methanogenesis and high-affinity CH_4 oxidation) with fewer mediating groups. We observed that finer scale processes can be more readily predicted from microbial community structure

than broader scale processes. In addition, the nature of those relationships differed, with broad processes limited by abundance while fine-scale processes were associated with diversity and composition. These findings demonstrate the importance of carefully defining the physiological scale of ecosystem function and performing community measurements that represent the range of possible controls on ecosystem processes.

INTRODUCTION

Belowground ecosystem processes can be highly variable, and there have been numerous attempts to explain or predict this variation using microbial community data. However, our ability to identify microbial community drivers of processes remains in its infancy. This challenge stems from at least three issues. First, community variables often have complex covariance structure (e.g. spatial or environmental autocorrelation) (Legendre, 1993), which can complicate the task of distinguishing the biotic signal underlying ecosystem process rate variation. Second, communities can control processes through a number of mechanisms, making the identification of these controls a challenge (Bier et al., 2015). For example, communities can influence the rate of a process through abundance (of particular groups or the community as a whole), composition (i.e. the identity of community members), diversity, and activity, each of which would require the quantification of different community attributes. Lastly, function is often assessed at a broad physiological scale that encapsulates many processes that could have unique controls (Inkpen et al., 2017). For example, gross decomposition of organic matter or net flux of methane (CH_4) into the atmosphere are commonly measured belowground ecosystem functions, yet these measurements represent the aggregate result of many different physiological processes.

We tested this idea using the two counteracting microbial processes that largely control atmospheric CH_4 emissions from soils: CH_4 production (methanogenesis) and CH_4 consumption (methanotrophy). Each of these processes can be further divided into underlying processes that involve fewer mediating

93 microbial taxa. For instance, gross methanogenesis can have direct inputs from at
94 least three processes: hydrogenotrophic (which uses CO_2 and H_2 to produce CH_4),
95 acetoclastic (which uses acetate), and/or methylotrophic (which uses methanol,
96 methyl-amides, or methyl-sulfides) methanogenesis. The process of methanotrophy
97 can be subdivided as well. Methanotrophy at high CH_4 concentrations (typical of
98 those found in waterlogged soil and sediment) is performed by a wide diversity of
99 methanotrophs found in the Gammaproteobacteria, Alphaproteobacteria, and
100 Verrucomicrobia (Knief, 2015), whereas the consumption of CH_4 at atmospheric
101 concentrations (a.k.a. high-affinity CH_4 oxidation) appears to be much more
102 phylogenetically restricted and is likely performed by many fewer taxa (Kolb, 2009;
103 Ho et al., 2013; Knief, 2015). Taken together, these observations suggest that gross
104 measurements of either methanogenesis or methanotrophy may mask subtle
105 variations in these underlying processes and could thereby blur the connection
106 between community variation and ecosystem function.
107 A major challenge in the study of ecosystem function lies in identifying
108 underlying community controls. Group abundance is one such form of control,
109 whereby the rate of a process only proceeds as quickly as the total number of
110 capable individuals. There are examples of this control for both methanogenesis (Ma
111 et al., 2012) and methanotrophy (Freitag & Prosser, 2009), but many studies have
112 found no such relationship (see Rocca et al., 2014). While this could be driven in
113 part by technical issues (e.g. abundance being inaccurately assessed due to primer
114 bias), processes may be controlled by other community attributes. Most soil
115 organisms are in an inactive state at any given time (Lennon and Jones, 2011). Low

activity levels can limit the rate of ecosystem processes either by decreasing syntrophic interactions or preventing substrate uptake. Measurements of methanotroph and methanogen transcriptional activity levels have been shown to positively correlate with process rates (Freitag & Prosser, 2009; Freitag et al., 2010), suggesting that the activity levels of key groups can constrain these processes. Moreover, community assessments using RNA may more closely approximate the active fraction of the community (Jones & Lennon, 2010; Kamke et al., 2010; Baldrian et al., 2012; although see Papp et al., 2018a) and therefore provide a means to approximate activity-based community controls.

The composition of a community can impose another constraint on ecosystem processes. Composition control (a.k.a. species identity effects (Bannar-Martin et al., 2018)) could occur if certain community members perform a process more efficiently or rapidly than others, and those taxa/traits are dispersal limited. In this case, certain individuals would be expected to more strongly correlate with process rate variation than others. Distinguishing such a compositional signal can be a challenge because communities tend to co-vary depending on their spatial proximity or similarity in environmental controls (Legendre, 1993). There is precedent to suggest that community composition is an important determinant of CH_4-cycling rates. For instance, even closely related methanogen/methanotroph taxa can differ in traits such as substrate affinity, substrate preference, environmental tolerance, or competitive ability (Garcia et al., 2000; Ho et al., 2013; Nazaries et al., 2013a; Knief, 2015). Therefore, differences in community composition have the potential to influence CH_4-cycling processes, which has been

139 shown in several systems (Bodelier et al., 2013; Nazaries et al., 2013b; McCalley et
140 al., 2014; Sierocinski et al., 2017, 2018). Membership of other functional guilds
141 within a community is also an important consideration, particularly for processes
142 that require metabolic byproducts as the primary substrate. Methanogens depend
143 on the fermentative byproducts (*e.g*. H^+ and acetate) of other community members
144 and must compete for these substrates with other community members. This is also
145 the case for methanotrophs, where competition for O_2 and/or other soil nutrients
146 can limit rates of methanotrophy (Bodelier et al., 2000). Thus, *who is there* may be a
147 particularly important consideration for predicting the rates of ecosystem
148 processes, particularly if efficient traits are dispersal limited or competition for
149 substrates is common.

150 Lastly, a growing body of work suggests that biodiversity may affect rates of
151 ecosystem processes (Tilman et al., 1996), as well as the resistance, resilience, or
152 stability of a process through time (Tilman & Downing, 1994; Loreau et al., 2001).
153 This pattern could arise through multiple ecological mechanisms including: 1) niche
154 complementarity, 2) sampling effects, or 3) facilitation. It has been argued that
155 ecosystem functions mediated by a wide assortment of taxa may be less influenced
156 by levels of diversity than those mediated by relatively fewer taxa (Schimel, 1995;
157 Schimel & Gulledge, 1998). This would suggest that as one narrows the
158 physiological scale of ecosystem function, the diversity of participants should
159 become a stronger determinant of process rates. The abilities to produce and
160 consume CH_4 are both highly phylogenetically conserved (Martiny et al., 2013), and
161 relatively few taxa possess the ability to carry out these processes. There are even

162 fewer taxa that perform underlying processes such as hydrogenotrophic
163 methanogenesis and high-affinity methanotrophy (Kolb, 2009; Knief, 2015). Positive
164 diversity – ecosystem function relationships have been observed for methanotrophy
165 experimentally using intact soil cores from the field (Bodelier et al., 2013), as well as
166 in artificially assembled methanotroph communities (Schnyder et al., 2018). This
167 has also been observed for methanogenesis in anaerobic digesters (Sierocinski et al.,
168 2018). Although several studies have tested whether diversity and process rates are
169 related, few have asked whether adjusting the physiological scale at which function
170 is assessed improves this relationship.

171 Here we present results from a set of experiments designed to identify the
172 biological drivers of variation in CH_4-cycling dynamics. Our goals were to determine
173 (1) whether we could identify significant community controls on CH_4 cycling after
174 accounting for covariance structure, and (2) whether the strength and nature of
175 those controls changes with the physiological scale of the process. To do this, we
176 collected soils along a diverse wetland-to-upland habitat gradient in the Congo
177 Basin, a region that has received very little scientific attention for its role in the
178 global CH_4 cycle (Bridgham et al., 2013; Kirschke et al., 2013) and has been shown to
179 exhibit highly dynamic spatial and temporal CH_4 cycling dynamics (Delmas et al.,
180 1992a, 1992b; Tathy et al., 1992; MacDonald et al., 1999). We estimate process rate
181 potentials under controlled laboratory conditions, which minimizes the impact of
182 environmental variation and enhances the biotic signal underlying process rate
183 variation. We varied the physiological scale at which we assessed ecosystem
184 function, ranging from broader scales including gross methanogenesis and

methanotrophy, to finer scales including hydrogenotrophic methanogenesis and high-affinity methanotrophy. We paired RNA- and DNA-based microbial community measurements with each process measurement and calculated four sets of community attributes (abundance, activity, composition, and diversity) to aid in the identification of putative community controls. We hypothesized that there would be a connection between microbial community structure and CH_4-cycling processes after accounting for environmental variation, and that finer scale processes (*i.e.* those involving a lower diversity of mediating taxa) would exhibit a stronger relationship with community attributes than broader processes, as exemplified by a higher proportion of variance explained. Our results suggest that communities are an important driver of CH_4-cycling processes in tropical ecosystems, and that the strength and nature of the relationship between community structure and ecosystem function can depend on the physiological scale by which function is assessed.

METHODS AND MATERIALS

Site selection and sampling

We selected a diverse set of 15 sites in Southwestern Gabon in and around the Gamba Complex of Protected Areas (Lee et al., 2006). Gabonese ecosystems belong to the Guineo-Congolian regional center of endemism (White, 1979), making them broadly representative of the Congo Basin. Our sites included 4 mineral-soil forested wetlands, 2 peatlands, 2 seasonally wet mineral-soil forests, 3 upland grasslands (2 with termite mounds), 2 upland forests, a 1-year old plantation, and 1

abandoned plantation. Seasonal wetlands were identified by tree species composition, thick O and/or A soil horizons with mottling, and tree watermarks. Water tables were at least 40 cm below the soil surface in seasonal wetlands. Our sampling took place at the beginning of the Gabonese rainy season, from October to November 2014.

Potential gross and high-affinity CH_4 oxidation rates

We collected three intact soil cores from above the water table at the beginning, middle, and end of 35 m field transects established at each site. The samples were stored in PVC tubes (5 cm dia., 8 cm height) to maintain soil structure and kept at *in situ* air temperatures (28 °C) until the end of the sampling trip (~3 weeks). One week after returning to the University of Oregon, each PVC core was placed into a gas-tight Mason jar that was retro-fitted with a headspace sampling port and incubated at 28 °C in the dark. Rates of aerobic CH_4 oxidation were determined under initially low (5 ppm CH_4/mL in headspace) and high (1000 ppm CH_4/mL headspace) CH_4 concentrations, to estimate rates of high-affinity and gross methanotrophy, respectively. CH_4 concentration measurements were taken at 0.33, 3, 6, and 9 hours for high-affinity methanotrophy and at 0.33, 3, 6, 9, 24, and 48 hours for gross methanotrophy. The same soil cores were used to determine high-affinity methane oxidation and gross methanotrophy in quick succession. We applied a first-order exponential decay function to determine the rate constant (k, units = d^{-1}; *i.e.* $dCH_4/dt = k[CH_4]$) of the exponential decrease in CH_4 when at low initial CH_4 concentrations (*i.e.* high-affinity methanotrophy). At high CH_4

concentrations we measured the linear decreases in CH_4 to determine the maximum velocity rates (V_{max}, units = μg CH_4 cm^{-3} d^{-1}) (*i.e.* gross methanotrophy). During our high-affinity CH_4 oxidation incubations, CH_4 concentrations exponentially decreased in all samples, except for one, across our four measurements; thus, all time points were included in subsequent calculations. While one sample did not immediately exhibit CH_4 oxidation at the first timepoint (0.33 hours), it did show exponential decreases in CH_4 concentrations following the 3 hour timepoint; thus, only three timepoints were used to calculate the k-value for this sample. During our gross methanotrophy incubations, we included only timepoints that encompassed the linear portion of the exponential decrease in CH_4 concentration, which ranged from 3-5 timepoints depending on the sample.

Potential gross methanogenesis and hydrogenotrophic pathway predominance

Across all wetland sites, we collected three intact soil cores in PVC tubes from 0 – 10 cm below the water table at the beginning, middle, and end of 35 m transects at each site. The samples were topped with site water and tightly sealed to ensure an anaerobic environment and transported to the University of Oregon. Anaerobic incubations took place at field temperatures (28 °C) within two days following arrival at University of Oregon. In a glove box filled with a N_2 atmosphere (<5% H_2 in the presence of palladium catalyst; Coy Laboratory Products, Grass Lake, Michigan, USA), approximately 10 g of wet weight soil were added to 120 mL serum bottles and mixed with 10 mL of deoxygenated, deionized water. Sample bottles were then flushed with N_2 for 15 minutes to begin the incubation. Headspace

254 samples were analyzed over the course of three days (0, 1, 2, and 3 days). Total CH_4
255 was calculated using Henry's Law, adjusting for solubility, temperature, and pH
256 (Bridgham & Ye, 2013). CH_4 production rates were calculated using the linear
257 accumulation ($r^2 > 0.90$ in all cases) of gas through time. To measure
258 hydrogenotrophic methanogenesis, we used a $^{14}CO_2$ tracer method (Keller &
259 Bridgham, 2007), which allowed us to distinguish the percent of total CH_4 that had
260 been produced using CO_2/H_2 as the substrate (i.e. hydrogenotrophic
261 methanogensis). This was done with a gas chromatograph fitted with a radioactive
262 gas proportional counter (LabLogic Systems) simultaneously with the gross
263 methanogenesis measurements over three days.
264
265 ***Soil physical and chemical analysis***
266 We measured a suite of abiotic variables from each soil sample to
267 incorporate into our community model as a covariate (see below). For the
268 methanogenesis study, we recorded pH, total % nitrogen (N), organic carbon (C),
269 moisture content, and bulk density. For the methanotrophy study, we measured N,
270 C, moisture content, and bulk density. Soil pH was determined from a 1:1 soil to
271 deionized water solution. Total % N and organic C were measured on a Costech ECS
272 4010 Elemental Analyzer (Valencia, CA), with each sample analyzed in duplicate.
273 Moisture content (gravimetric water content) and bulk density were measured by
274 the change in weight of a soil sub-sample following 48 hours of drying at 60 °C.
275 Additionally, material from the three soil cores at each site was combined and
276 homogenized for texture analysis using the hydrometer method (Gavlak et al.,

277 2003), with 5% sodium hexametaphosphate as the dispersing solution. Because soil
278 texture measurements required pooling samples from each site- and all other
279 variables were measured on a per sample basis, texture was not included in the
280 environmental covariate calculation.
281
282 ***Soil RNA/DNA co-extraction and sequencing***
283 Soil DNA and RNA were co-extracted from Lifeguard-preserved soil samples
284 using MoBio's Powersoil RNA Isolation kit with the DNA Elution Accessory Kit
285 (MoBio, California, USA) following manufacturer's instructions. RNA was reverse
286 transcribed to cDNA using Superscript III first-strand reverse transcriptase and
287 random hexamer primers (Life Technologies, USA). Extractions were quantified
288 using Qubit (Life Technologies, USA). We amplified the V4 region of the 16S SSU
289 rRNA gene in sample DNA and cDNA using the primers 515F and 806R (Caporaso et
290 al., 2011). Sequencing libraries were prepped using a dual-indexing approach
291 (Kozich et al., 2013; Fadrosh et al., 2014). In short, each PCR reaction was
292 performed using 12.5 µl NEBNext Q5 Hot Start HiFi PCR master mix (New England
293 Biolabs, USA), 11.5 µl gene-specific primer mix (1.09 µM of each primer), and 1 µl
294 template (DNA or cDNA). A subset of samples was used to find 1) the optimal primer
295 annealing temperature, and 2) the minimum number of cycles for adequate target
296 amplification. For the 16S rRNA gene target this was 61° C and 20 cycles. The final
297 reaction conditions were: 98° C 30 seconds (initialization), 98° C 10 seconds
298 (denaturation), gene-specific annealing step for 20 seconds (see above), and 72° C
299 for 20 seconds (final extension). Reactions were followed by magnetic bead

300 purification using 20 µl Mag-Bind RxnPure Plus isolation beads (Omega Bio-Tek,
301 USA). Reactions were quantified using Qubit (Life Technologies, USA) then were
302 multiplexed at equimolar concentration. Final pooled amplicon libraries were
303 sequenced using the Illumina MiSeq (300 paired-end) platform at the Oregon State
304 University Center for Genome Research and Biocomputing facility.
305
306 ***Bioinformatic processing***
307 Demultiplexed reads were joined using PEAR (version 0.9.10) with default
308 parameters (Zhang et al., 2014) and quality filtered using Prinseq (version 0.20.4)
309 (Schmieder & Edwards, 2011). Sequences with a mean quality score ≥ 30 and length
310 250-350 bp were retained. Sequences were dereplicated, denoised, and checked for
311 chimeras using the DADA2 pipeline (Version 1.6) (Callahan et al., 2016)
312 implemented in QIIME2 (Caporaso et al., 2010) (https://qiime2.org). For the
313 methanogenesis study 17 of the 18 DNA-based samples, and 13 of the 18 RNA-based
314 samples had sufficient quality to be included. For the methanotrophy study 41 of the
315 44 DNA-based samples, and 34 of the 44 RNA-based samples passed our quality
316 filter. Taxonomy was assigned to the resulting amplicon sequence variants (ASVs)
317 using the Ribosomal Database Project online classifier (Wang et al., 2007) with
318 database release 11.5 (Cole et al., 2014).
319
320 ***Quantitative PCR***
321 We quantified the abundance of methanogens in each sample from which
322 CH_4 production and hydrogenotrophic pathway predominance were measured. To

323 do so we performed qPCR of the *mcrA* gene on sample DNA using the mlas-mcrA-rev
324 primer combination (Steinberg & Regan, 2008). Samples were run on an ABI
325 StepOnePlus thermocycler (ABI, USA), using Kapa SYBR reagents (Kapa Biosystems,
326 USA) according to manufacturer recommendations. For each sample, 8 ng DNA was
327 used, and the following amplification conditions were applied following
328 optimization: 98° C 10 minutes, 98° C 15 seconds, 55.6° 15 seconds, 72° 60 seconds.
329 A melt curve analysis was performed to verify target amplification. Not all samples
330 reliably amplified; in the end we obtained useable *mcrA* quantifications for 12 of the
331 18 samples. Although attempted, the transcriptional activity of *mcrA* from soil cDNA
332 did not produce reliable results, and thus is not included in this study. We used a
333 similar approach to quantify methanotroph abundance and transcriptional activity
334 by targeting the *pmoA* gene in the sample DNA and cDNA, respectively, using the
335 A189 – mb661 primer combination (Bourne et al., 2001). Reactions were performed
336 on a Bio-Rad CFX96 real-time qPCR instrument, using SsoAdvanced Universal SYBR
337 Green supermix (Bio-Rad, USA) following manufacturer instructions. For each
338 sample, 2 ng template were used with the following reaction conditions: 98° C 10
339 minutes, 98° C 15 seconds, 55.6° 15 seconds, 72° 60 seconds. All samples were
340 amplified in triplicate. In both cases, sample amplification was compared to a
341 standard positive control to quantify total gene (or transcript) copy number. We
342 obtained useable *pmoA* quantifications for 42 of the 44 DNA samples and 32 of the
343 44 RNA samples. In the case of *mcrA*, the positive control was an *mcrA* plasmid and,
344 in the case of *pmoA*, we used purified DNA from strain *Methylococcus capsulatus*
345 Foster and Davis (ATCC 33009D-5). We used LinRegPCR (Ramakers et al., 2003;

346 Ruijter et al., 2009) to process amplification data which allows for the calculation of
347 individual PCR efficiencies. Individual PCR efficiencies did not significantly differ
348 between habitat types, so gene copy was calculated using the average PCR efficiency
349 of all reactions. Finally, gene copy (or transcript) numbers were normalized to the
350 total ng DNA (or cDNA) used in the reaction.
351
352 ***Microbial community attribute calculations, statistical analysis, and***
353 ***comprehensive modeling***
354 All statistical analyses were performed using R (version 3.4.4) (R Core Team,
355 2018). Community matrices for the methanotrophy experiments were rarefied ten
356 times at 28,000 counts per sample, then averaged, and community matrices for the
357 methanogenesis experiments were rarefied to 30,400 counts per sample ten times
358 and averaged, in order to account for differences in sampling extent across samples.
359 Additionally, these rarefied community matrices were subsetted for known
360 methanogens/methanotrophs (Supplementary Table 1) to create functional group
361 community matrices. We categorized community data into the following four
362 attributes (Table 1): 1) *Abundance* of methanogens/methanotrophs using qPCR of
363 *mcrA* and *pmoA* genes (described above) respectively, as well as the relative
364 abundance of known methanogens/methanotrophs in the DNA-inferred 16S-based
365 prokaryotic community, 2) *Activity* of methanogens/methanotrophs using the
366 relative abundance of methanogens and methanotrophs in the RNA-inferred
367 prokaryotic community, and qPCR of *pmoA* using soil cDNA (described above), 3)
368 *Composition* of the broader prokaryotic community or of subsets of known

369 methanogen/methanotroph taxa from the 16S-inferred community matrix
370 (described below), and 4) *Diversity* of the prokaryotic community as well as
371 methanogen/methanotroph community subsets using ASV-level richness and
372 Shannon diversity. Species richness and Shannon diversity were calculated using
373 the 'vegan' package (Oksanen et al., 2015) in R. Regression plots were created using
374 the package 'ggplot2' (Wickham, 2009), and 95% confidence interval bands were
375 plotted around each linear fit using the 'geom_smooth' function (option = 'lm').
376 Difference in process rates among wetlands and uplands was assessed using a
377 Kruskal-Wallis test.
378
379 *Associations between community attributes and CH_4-cycling processes*
380 Because communities tend to have complex covariance structure, we took
381 several measures to avoid spurious associations when distinguishing biotic
382 correlates of CH_4-cycling processes. First, our process measurements were
383 performed under constant temperatures similar to those experienced in the field
384 (described above). By doing so, we minimized the influence of certain
385 environmental factors (*e.g.* temperature fluctuations or precipitation events) on our
386 process rate measurements. Secondly, we added two covariates to our model when
387 assessing associations with process rate measurements: 1) a soil physicochemical
388 covariate, and 2) and a sample (community) covariate. The soil physicochemical
389 covariate was calculated using principle components analysis (PCA) on soil
390 physicochemical measurements (described above). This was done using the prcomp
391 function in the 'stats' package of R (R Core Team, 2018), with variables scaled to

392 unit variance to account for differences in units of measurement. Sample scores for
393 the first principle component (PC1) were used as the environmental covariate. We
394 applied a similar approach to calculate the community covariate. In this case, the
395 rarefied community matrix was Hellinger transformed, then ordinated using the
396 prcomp function while scaling to unit variance, in order to calculate the community-
397 based sample PC1 scores. By including these covariates in our model we are
398 regressing each community attribute against the residual variation of the CH_4-
399 cycling process of interest after accounting for the variation explained by
400 environment and underlying sample structure.

401 To assess associations between community membership and process rate
402 variation we used the regression approach described above on the relative
403 abundance of individual taxa (ASVs). Since performing this type of analysis on
404 thousands of individual taxa increases the risk of false positives, we adjusted our
405 significance threshold (alpha = 0.05) using a Bonferroni correction, i.e. by dividing
406 by the number of of taxa being tested. In cases where significant taxa were
407 identified, those taxa were subsetted from the rarefied community matrix, then
408 ordinated (following the above procedure) to reduce them to a single variable. The
409 sample scores of the first principle component were subsequently used for
410 regression against CH_4-cycling process rates. Linear regressions were performed
411 using the lm function in the 'stats' package in R. Gross methanotrophy and
412 methanogenesis rate data were $\log_2$-transformed in order to satisfy assumptions of
413 normality. For each relationship we report the adjusted R^2 and *p* value.
414

415 RESULTS

416 ***Identifying biotic drivers of CH_4-cycling processes***

417 ***Methanogenesis processes***

418 *Gross Methanogenesis*

419 Gross methanogenesis rates varied from 0.06 to 6.7 μmol CH_4 g soil^{-1} d^{-1}
420 (average 1.1 ± 1.5 μmol CH_4 g soil^{-1} d^{-1}, Fig. 1A), with rates in mineral soil wetlands
421 on average 3.8 times higher than peatlands. For breakdown of soil physico-chemical
422 variables by habitat see Supplementary Table 2. We identified two community
423 attributes that were associated with gross methanogenesis rate after accounting for
424 sample and environmental covariance structure: methanogen abundance (*i.e.* the
425 abundance of *mcrA* genes, Adj. R^2 = 0.47, p = 0.008, Fig. 1B, Table 2), and the alpha
426 diversity of methanogens (Richness: Adj. R^2 = 0.25, p = 0.023, Shannon: Adj. R^2 =
427 0.23, p = 0.029). Both relationships were positive, suggesting that more abundant
428 and/or diverse populations of methanogens are associated with higher rates of
429 gross methanogenesis. We did not identify any individual prokaryotic taxa that were
430 significantly associated with gross methanogenesis after accounting for
431 environmental and sample covariance and adjusting for multiple comparisons. Soil
432 pH was the only significant abiotic predictor of methanogenesis (Adj. R^2 = 0.24, p =
433 0.023), showing a positive relationship whereby values approaching neutral pH had
434 higher rates of methanogenesis.

435

436

437

438 *Hydrogenotrophic methanogenesis*

439 The most pronounced difference in the predominance of the
440 hydrogenotrophic pathway was between mineral soil wetlands and peatlands,
441 where it accounted for 30.7 ± 11.2 % and 76.7 ± 23.0 % of total methanogenesis,
442 respectively (Fig. 1C). We identified a negative relationship between the DNA-
443 inferred alpha diversity of the methanogens and the predominance of the
444 hydrogenotrophic pathway (Shannon: Adj. R^2 = 0.710, p < 0.001 Fig. 1D, Table 2,
445 Richness: Adj. R^2 = 0.455, p = 0.002). We also identified a negative relationship with
446 the RNA-inferred alpha diversity of the prokaryotic community (Shannon: Adj. R^2 =
447 0.609, p = 0.001). The only abiotic variables that were significantly associated with
448 hydrogenotrophic methanogenesis were a negative relationship with soil pH (Adj.
449 R^2=0.32, p < 0.01), and a positive relationship with soil C (Adj. R^2=0.341, p < 0.01).
450

451 ***Methanotrophy processes***

452 *Gross methanotrophy*

453 Average rates of gross CH_4 consumption (V_{max}) were higher in wetland sites
454 (including seasonal wetlands) (0.3 ± 0.05 μmol CH_4 g soil^{-1} d^{-1}) than upland sites
455 (0.1 ± 0.02 μmol CH_4 g soil^{-1} d^{-1}) (Fig. 2A, Kruskal-Wallis: Chi-squared = 6.85, df = 1,
456 p = 0.008), and significantly correlated with every abiotic variable measured. Gross
457 methanotrophy rates were negatively correlated with soil bulk density (Adj. R^2=
458 0.135, p =0.008). Note that the inverse of V_{max} is presented, i.e. higher uptake rates
459 are represented by higher values. Conversely gross methanotrophy rates were
460 positively correlated with soil moisture (Adj. R^2= 0.22, p < 0.001), soil C (Adj. R^2=

461 0.094, p =0.024), and soil N (Adj. R^2= 0.105, p =0.02). The only community attribute
462 that correlated with gross methanotrophy after accounting for variation due to soil
463 physicochemical variables was methanotroph abundance (i.e. *pmoA* copy number,
464 Adj. R^2=0.139, p=0.01, Fig. 2B, Table 2).
465
466 *High-affinity methanotrophy*
467 Of the four processes measured, high-affinity methanotrophy was the only
468 process to exhibit composition-based control involving the broader prokaryotic
469 community beyond known methanotrophs. Rates of high-affinity methane oxidation
470 varied considerably across our samples (range -9.15 to 2.08) (Fig. 2C) and were
471 higher in upland sites relative to wetland sites (including seasonal wetlands)
472 (Kruskal-Wallis: Chi-squared = 11.52, df = 1, $p < 0.001$). After accounting for sample
473 and environmental covariance, we identified 11 taxa in the DNA-inferred
474 community and 5 taxa in the RNA-inferred community whose relative abundance
475 significantly corresponded to high-affinity methanotrophy rates. The finest level of
476 taxonomic assignment for these taxa varied from order to genus. DNA-inferred taxa
477 identified included members of the genera *Nitrosphaera* (Thaumarchaeota),
478 *Roseiarcus* (Alphaproteobacteria), *Aminiphilus* (Synergistetes), and *Acidisoma*
479 (Alphaproteobacteria), a member of the family Thermosporaceae (Actinobacteria),
480 four members of Acidobacteria Group 2, and two members of Acidobacteria Group 6
481 (Table 3). There was no ASV-level overlap with the RNA-inferred taxa that were
482 identified. The RNA-inferred taxa included members of the genera *Beijerinckia*
483 (Alphaproteobacteria), *Deferrisoma* (Deltaproteobacteria), *Nitrospirillum*

484 (Alphaproteobacteria), the family Thermonosporaceae (Actinobacteria), and a
485 member of Acidobacteria Group 1 (Supplementary Table 3).
486 We next ordinated the relative abundances of these taxa to reduce them to a
487 single variable. The first principle component of both of these community subsets
488 significantly correlated with high-affinity methanotrophy (RNA-inferred PC1 axis:
489 Adj. $R^2 = 0.647$, $p < 0.001$, Fig. 2D, Table 2, DNA-inferred PC1 axis: Adj. $R^2 = 0.583$, p
490 < 0.001). Lastly, we tested if high-affinity methanotrophy correlated with any other
491 community attributes. After accounting for covariance structure, there were no
492 other biotic correlates of high-affinity methanotrophy beyond composition-based
493 variables.
494
495 DISCUSSION
496 *The utility of microbial community attributes in predicting function*
497 The utility of conventional microbial community measurements for
498 predicting ecosystem functions has been recently called into question (Graham et
499 al., 2014; Rocca et al., 2014; Inkpen et al., 2017; Louca et al., 2018). Here we argue
500 that many of the difficulties associated with detecting community structure –
501 ecosystem function relationships could be overcome with careful consideration of
502 the community attributes chosen, the physiological scale of functional assessment,
503 and how environmental variation is controlled. In this study we have addressed
504 each of these concerns. Our work demonstrates 1) that there is a connection
505 between communities and ecosystem processes after accounting for variation due
506 to external factors, and 2) that the strength, as well as the nature, of the relationship

507 between communities and ecosystem function depends on the physiological scale of
508 the function.

509 Ecosystem function measurements face issues of physiological scale (Inkpen
510 et al., 2017), i.e. they represent the aggregate result of numerous underlying
511 processes. Detecting a causal link between community measurements and
512 ecosystem function thus becomes increasingly difficult for functions that include
513 inputs from multiple processes. This suggests that as one narrows the functional
514 scale to a level that more closely approximates individual physiologies, the strength
515 of the relationship with the community should increase. Our study supports this
516 hypothesis. For both methanogenesis- and methanotrophy-related processes, a
517 similar trend emerged; broader-scale functions had a weaker relationship with
518 community attributes than finer-scale functions. For instance, the best predictor of
519 gross methanogenesis was methanogen abundance (i.e. *mcrA* copy number),
520 explaining 47% of the variance, whereas hydrogenotrophic methanogensis – which
521 represents a finer physiological scale– showed the strongest association with
522 methanogen alpha diversity, explaining 71% of the variance (Table 2). For
523 methanotrophy processes, gross methanotrophy was best predicted by
524 methanotroph abundance (i.e. *pmoA* copy number), but this connection was quite
525 weak and only explained ~14% of the variance. By contrast, much more of the
526 variance in high-affinity methanotrophy could be explained by RNA-inferred
527 community composition (~64%, Table 2). While our specific hypothesis only
528 represents two processes for each type of function, our results provide support for
529 the idea that the physiological scale of function is an important consideration for

530 community structure-ecosystem function studies. Future work could extend the
531 generality of our findings by assessing an even wider assortment of physiological
532 scales (e.g. net CH_4 flux) or by extending this framework to other ecosystem
533 functions (e.g. soil respiration).
534
535 *Developing community variables that represent putative process controls*
536 Communities can control processes in several distinct ways. It is therefore
537 important that the variables we choose to represent communities reflect these types
538 of control. One key finding from our work was that broader scale processes had
539 distinctly different predictors than the underlying finer scale processes. Hence,
540 several of the relationships uncovered by our work would have gone undetected
541 had we focused solely on a single attribute. Both gross methanogenesis and
542 methanotrophy were best predicted by abundance-based variables (i.e. *mcrA* and
543 *pmoA* copy number, respectively), suggesting that these processes could be limited
544 by the total number of individuals capable of performing them. Similar relationships
545 between abundance and methanotrophy/methanogenesis rates have been reported
546 (Freitag & Prosser, 2009; Ma et al., 2012), although a number of studies have
547 demonstrated no such relationship (see Rocca et al., 2014) – suggesting other
548 important controls. Hydrogenotrophic methanogenesis and high-affinity
549 methanotrophy – the finer-scale processes – by contrast were best predicted by
550 diversity and composition measures, respectively. Hydrogenotrophic predominance
551 was inversely related to methanogen diversity. One possible explanation for this
552 relationship is that more diverse methanogen consortia would be more likely to

553 contain other methanogen functional groups (*e.g.* acetoclastic or methylotrophic
554 taxa), which would thus affect the relative contribution of the hydrogenotrophic
555 pathway to gross methanogenesis.

556 The strongest – and only – biotic variables associated with high-affinity
557 methanotrophy were based on RNA- and DNA-inferred composition (i.e. taxon
558 identity), suggesting that trait differences among taxa could be especially important
559 for this process. Interestingly, none of the associated taxa we identified were known
560 methanotrophs. This insight highlights the importance of not restricting our search
561 to taxa that are canonically associated with methanotrophy. While there are issues
562 with the commensurability of taxonomic composition and ecosystem function
563 (Inkpen et al., 2017), these taxa could still be causally linked to high-affinity
564 methanotrophy in at least two ways. First, at least some could be non-canonical
565 methanotrophs that are consuming CH_4. Even though the ability to consume CH_4 is
566 conserved phylogenetically (Martiny et al., 2013), canonical methanotrophs (as well
567 as high affinity methanotrophs) are nevertheless polyphyletic (Knief, 2015),
568 suggesting that methanotrophy has evolved multiple times or has been laterally
569 transferred. Another possibility is that these taxa influence methanotrophy through
570 ecological interactions with methanotrophs (e.g. competition or facilitation). A final
571 possibility is that these taxa are simply a marker for high-affinity methanotrophy,
572 co-varying with a variable that is causally linked. One of the DNA-inferred taxa
573 identified, *Nitrosphaera sp.* (Thaumarchaeota), is a known ammonia oxidizer.
574 Ammonia monooxygenase and methane monooxygenase are phylogenetically
575 related (Holmes et al., 1995), and it has been suggested that ammonia oxidizers may

576 be able to bind CH_4 (Arp et al., 2002; Ross & Rosenzweig, 2017). Another taxon,
577 *Roseiarcus* (Alphaproteobacteria), is closely related to alphaproteobacterial
578 methanotrophs and has been isolated from a methanotrophic consortium enriched
579 from *Sphagnum* peat (Kulichevskaya et al., 2014). Thus, *Roseiarcus* could be either
580 directly consuming CH_4, or interacting with methanotrophs. Two of the RNA-
581 inferred taxa, *Nitrospirillum* and *Beijerinckia* (both Alphaproteobacteria), are
582 diazotrophs and could thus influence methanotroph activity by fixing atmospheric
583 N_2. The influence of other correlated taxa on methanotrophy is less clear, but
584 competition for soil nutrients/O_2, facilitation, or simply acting as a marker remain
585 possibilities.

586 While we attempted to equally represent each attribute in our modeling,
587 activity-based attributes were under-represented in this study. Transcriptional
588 levels of *pmoA* and *mcrA* have been used as proxies for methanotroph/methanogen
589 activity in a variety of studies (Chen et al., 2007; Freitag & Prosser, 2009; Freitag et
590 al., 2010). While we successfully quantified *pmoA* transcriptional activity, our
591 attempt to do so for *mcrA* was problematic. This was not likely due to a lack of
592 activity of methanogens (since CH_4 was continuously produced throughout the
593 experiment), but rather due to PCR inhibitors such as humic substances present in
594 organic-rich soils. We took our community inference methods a step further than
595 many other studies by using both RNA- and DNA-based 16S rRNA profiling. It has
596 been established that the relative abundances of taxa in the RNA-inferred
597 community should not be used as a direct assessment of activity levels (Papp et al.,
598 2018a, 2018b). However, it is likely that the RNA-inferred community is at least

599 enriched for the active fraction of soil taxa relative to the DNA-inferred community
600 (which could contain higher proportions of inactive, dormant, or dead individuals)
601 (Lennon & Jones, 2011). Thus, by including RNA-based community inference we
602 were able to use an additional window onto the community that could have
603 functional relevance.
604
605 *Gaining a better understanding of tropical CH_4 dynamics*
606 Despite the established importance of tropical ecosystems as global CH_4
607 sources (Kirschke et al., 2013; Sjögersten et al., 2014), our understanding of the
608 ecological controls over CH_4-cycling throughout these regions remains limited
609 (Bridgham et al., 2013). The majority of studies aimed at identifying controls on
610 CH_4-cycling dynamics have been performed in higher latitude ecosystems such as
611 northern peatlands (Bridgham et al., 2013). The contribution of biotic variables to
612 CH_4-cycling dynamics may be a more important determinant of variation across
613 tropical environments relative to higher latitudes. Methanogen population growth
614 rates are slow because all methanogenic pathways have very low thermodynamic
615 yields that are often barely above the threshold for growth under *in-situ* conditions
616 (Conrad, 1999; Megonigal et al., 2004). Thus, methanogens inhabiting high latitude
617 environments must recover each season from freeze-thaw events and will exhibit
618 low levels of activity/growth until warmer temperatures are reached. In tropical
619 ecosystems where prolonged freezing conditions are essentially absent, trait-level
620 distributions of CH_4-cycling taxa could play a stronger role regulating spatial
621 differences in CH_4 dynamics. While our study was not designed to compare

differences between high- and low-latitude ecosystems, an interesting trend that emerged from our results was that abiotic variables tended to be less predictive of CH_4 cycling relative to biotic variables (with the exception of gross methanotrophy). Importantly, our laboratory incubations deliberately downplayed the influence of several key environmental factors (*e.g.* temperature fluctuations or rainfall events) that could influence CH_4-cycling rates. Nevertheless, most of our environmental variables were independent from our incubation conditions (*e.g.* %C, %N, pH, soil bulk density), and each only explained a relatively small fraction of the variance. Thus, an important outstanding question is whether the strength and nature of biotic controls on CH_4-cycling dynamics differs between high- and low-latitude ecosystems.

Conclusion

How communities map onto ecosystem function is a widely debated topic. Central to this debate are issues related to the physiological scale of function, the identification of useful community attributes, and accounting for the underlying influence of the environment. Our study provides two unique perspectives to this debate. First, we suggest that broad definitions of function could be obscuring the connections with community attributes. Secondly, by compiling community attributes according to their putative role in controlling processes, we show that finer scale processes may face controls that differ from those of the coarser processes to which they contribute. Collectively, these findings demonstrate the importance of carefully defining the physiological scale of ecosystem function and

performing community measurements that represent putative controls on ecosystem processes.

ACKNOWLEDGEMENTS

We thank the Government of Gabon, Centre National de la Recherche Scientifique et Technologique for permission (Permit No AR0035/14/MESRS/CENAREST/CG/CST/CSAR) to conduct this study. We thank F. Bivigou, H. Memiaghe, L. Tchignoumba, E. Tobi, I. Akendengue for their help collecting samples. The University of Oregon, the Gabon-Oregon Transnational Center on Environment and Development, the Smithsonian Conservation Biology Institute, and Shell Gabon provided financial and logistical support. BB and KM are grateful for support by the National Science Foundation – Dimensions of Biodiversity program (DEB 14422214), and SB and AH are grateful for support by the Office of Biological and Environmental Research, Terrestrial Ecosystem Science Program, U.S. Department of Energy (DE-SC0008092 and DE-39SC0012088).

FIGURES AND TABLES

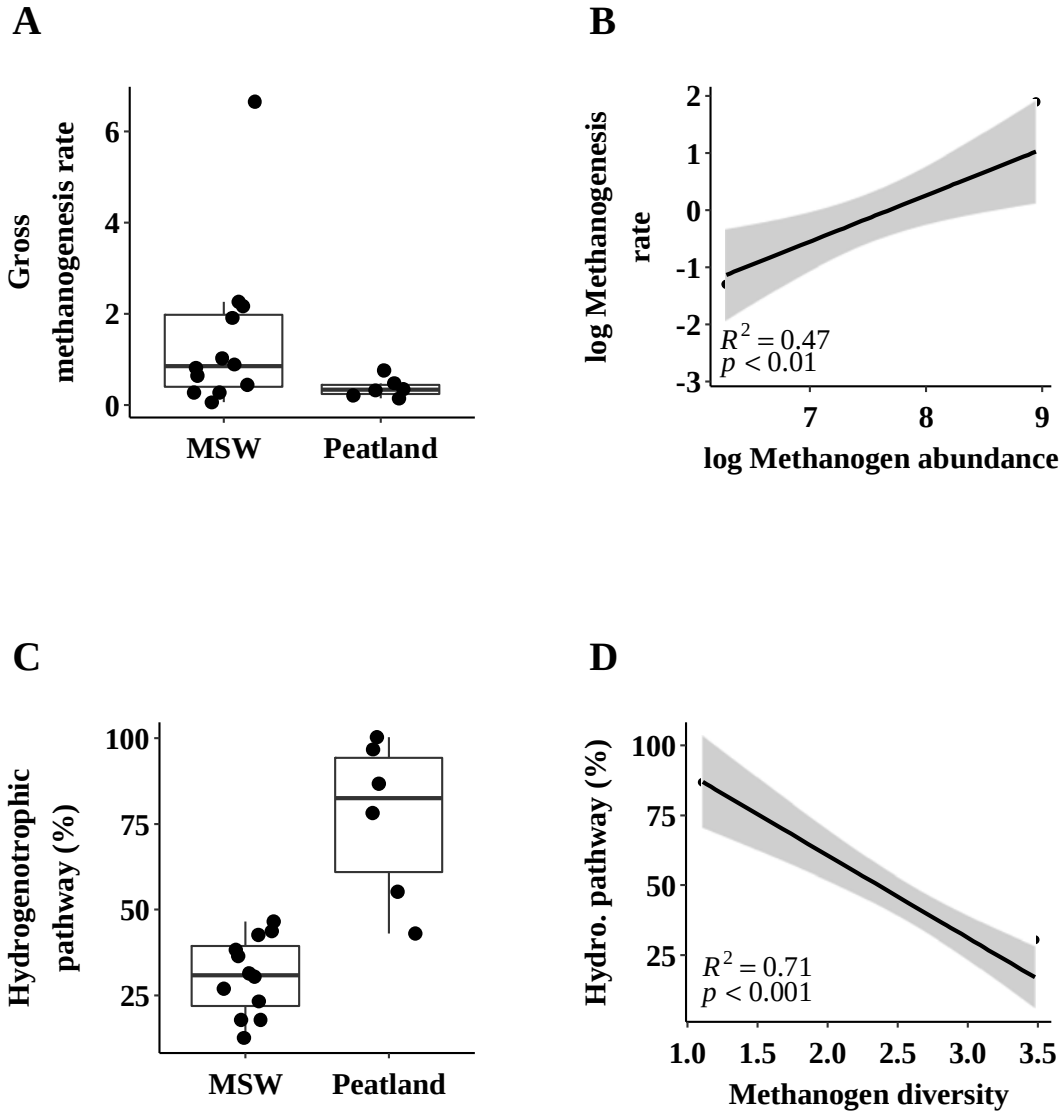

Fig. 1: The rates and biotic drivers of methanogenesis-related processes across Congo Basin wetlands. A) Methanogenesis rate (μmol CH_4 g $soil^{-1}$ d^{-1}) across the two wetland habitats. MSW = mineral soil wetland. B) The log_2 methanogenesis rate is best predicted by log_2 methanogen abundance (qPCR of *mcrA* gene). C) The predominance (%) of the hydrogenotrophic pathway in gross methanogenesis across wetland habitats. D) Hydrogenotrophic pathway predominance is inversely related to the alpha diversity (Shannon index) of the methanogen community. Each point represents an individual soil sample. Gray bands represent 95% confidence intervals of the linear model.

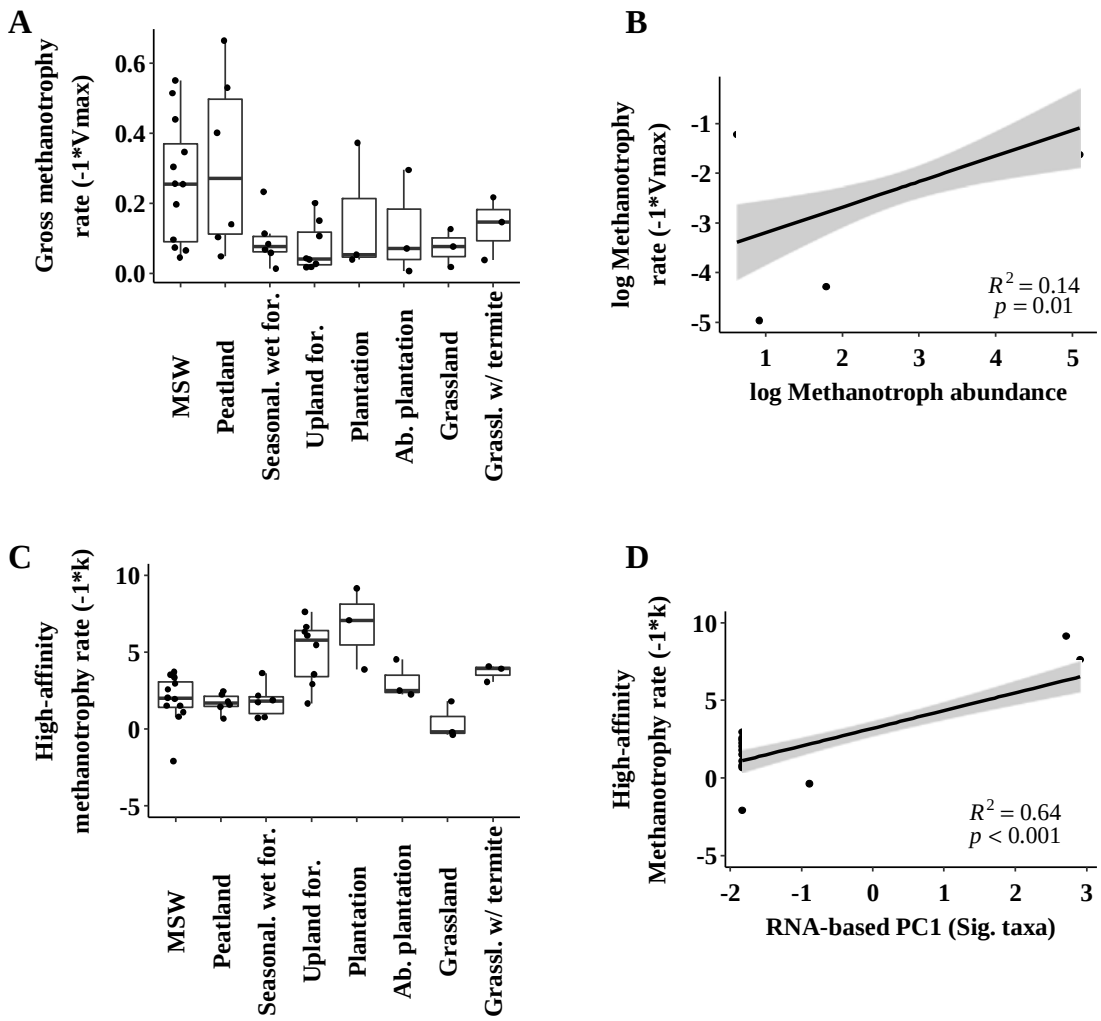

Fig. 2 The rates and biotic drivers of methanotrophy-related processes across Congo Basin habitats. Note the inverse of V_{max} and k and presented so that higher positive values correspond to higher rates of uptake. A) Gross methanotrophy rate (-1* V_{max}) across habitats. MSW = mineral soil wetland, Seasonal. Wet for. = seasonally inundated forest, Upland for. = upland forest, Ab. plantation = abandoned plantation, Grassland w/ termite = grassland habitat dominated by termite mounds. B) Gross methanotrophy rate is positively related to the $\log_2$ abundance of methanotrophs (*pmoA* gene copy number). C) High-affinity methanotrophy rate across habitats. D) High-affinity methanotrophy rates are best predicted by the first principle component (PC1) of a subset of significantly associated taxa (Sig. taxa) identified in the RNA-inferred prokaryotic community. Gray bands represent 95% confidence intervals of the linear model.

695 **Table 1:** The community attributes calculated in this study used to identify putative
696 community controls on process rates.

Attribute	Variables
Abundance	qPCR (of *mcrA* & *pmoA* genes)
	Relative abundance (in DNA-inferred prokaryotic community) of methanogens/methanotrophs
Activity	cDNA qPCR (pmoA)
	Relative abundance (in RNA-inferred prokaryotic community) of methanogens/methanotrophs
Composition	Matrix of 16S-based prokaryotic community inferred from RNA
	Matrix of 16S-based prokaryotic community (DNA-inferred)
	Matrix of methanogen/methanotroph taxa subsetted from 16S-based matrix (DNA-inferred)
	Species (ASV) richness of RNA/DNA-inferred prokaryotic community
Diversity	ASV richness of methanogen/methanotroph community subsets (RNA & DNA)
	Shannon (ASV) diversity of RNA/DNA-inferred prokaryotic community
	Shannon diversity of methanogen/methanotroph community subsets (RNA & DNA)

697

698

699

700

701

702

703

704

705

706

707

708 **Table 2:** Narrow scale processes have a higher association with community
709 attributes. Process assessment scale: whether a process assessment is the aggregate
710 result of several processes (broad) or only one (fine). Adj. R^2 = the proportion of the
711 variance explained by the attribute.
712

	Physiological scale of process	Best fit community attribute	Adj. R^2	*P* value
Methanotrophy processes				
Gross Methanotrophy (V_{max})	Broad	Abundance (*pmoA* copy)	0.14	0.01
High affinity methanotrophy (k)	Fine	Composition (RNA-inferred)	0.64	< 0.001
Methanogenesis processes				
Gross Methanogenesis (µmol CH_4 g soil^{-1} d^{-1})	Broad	Abundance (*mcrA* copy)	0.47	0.008
Hydrogenotrophic methanogenesis (% gross CH_4 production)	Fine	Diversity (methanogens)	0.79	< 0.001

713

714 DATA ACCESSIBILITY

715 Sequence data, sample meta data, biogeochemical data, ASV community matrices

716 and R script for analysis will be made available upon acceptance of publication.

717

718 AUTHOR CONTRIBUTIONS

719 KM, AH, SB and BB designed and performed research. KM, AH, AK, and AM analyzed

720 data. KM wrote the paper with contributions from all authors.

721

722

723

724

725

726 REFERENCES

727 Arp D.J., Sayavedra-Soto L.A., & Hommes N.G. (2002) Molecular biology and
728 biochemistry of ammonia oxidation by Nitrosomonas europaea. *Arch.*
729 *Microbiol.*, **178**, 250–255.
730 Baldrian P., Kolařík M., Stursová M., Kopecký J., Valášková V., Větrovský T., Zifčáková
731 L., Snajdr J., Rídl J., Vlček C., & Voříšková J. (2012) Active and total microbial
732 communities in forest soil are largely different and highly stratified during
733 decomposition. *ISME J.*, **6**, 248–58.
734 Bannar-Martin K.H., Kremer C.T., Ernest S.M., Leibold M.A., Auge H., Chase J.,
735 Declerck S.A., Eisenhauer N., Harpole S., Hillebrand H., Isbell F., Koffel T., Larsen
736 S., Narwani A., Petermann J.S., Roscher C., Cabral J.S., & Supp S.R. (2018)
737 Integrating community assembly and biodiversity to better understand
738 ecosystem function: the Community Assembly and the Functioning of
739 Ecosystems (CAFE) approach. *Ecol. Lett.*, **21**, 167–180.
740 Bier R.L., Bernhardt E.S., Boot C.M., Graham E.B., Hall E.K., Lennon J.T., Nemergut
741 D.R., Osborne B.B., Ruiz-González C., Schimel J.P., Waldrop M.P., & Wallenstein
742 M.D. (2015) Linking microbial community structure and microbial processes:
743 An empirical and conceptual overview. *FEMS Microbiol. Ecol.*, **91**, 1–11.
744 Bodelier P.L.E., Meima-Franke M., Hordijk C. a, Steenbergh A.K., Hefting M.M.,
745 Bodrossy L., von Bergen M., & Seifert J. (2013) Microbial minorities modulate
746 methane consumption through niche partitioning. *ISME J.*, **7**, 2214–28.
747 Bodelier P.L.E., Roslev P., Henckel T., & Frenzel P. (2000) Stimulation by ammonium-
748 based fertilizers of methane oxidation in soil around rice roots. *Nature*, **403**,
749 421–424.
750 Bourne D.G., Donald I.A.N.R.M.C., & Murrell J.C. (2001) Comparison of pmoA PCR
751 Primer Sets as Tools for Investigating Methanotroph Diversity in Three Danish
752 Soils. *Appl. Environ. Microbiol.*, **67**, 3802–3809.
753 Bridgham S.D., Cadillo-Quiroz H., Keller J.K., & Zhuang Q. (2013) Methane emissions
754 from wetlands: Biogeochemical, microbial, and modeling perspectives from
755 local to global scales. *Glob. Chang. Biol.*, **19**, 1325–1346.
756 Bridgham S.D. & Ye R. (2013) Organic Matter Mineralization and Decomposition.
757 *Methods in Biogeochemistry of Wetlands* (ed. by R.D. DeLaune, K.R. Reddy, C.J.
758 Richardson, and J.P. Megonigal), pp. 385–406. SSSA, Madison, WI.
759 Callahan B.J., McMurdie P.J., Rosen M.J., Han A.W., Johnson A.J.A., & Holmes S.P.
760 (2016) DADA2: High-resolution sample inference from Illumina amplicon data.
761 *Nat. Methods*, **13**, 581.
762 Caporaso J.G., Kuczynski J., Stombaugh J., Bittinger K., Bushman F.D., Costello E.K.,
763 Fierer N., Gonzalez Peña A., Goodrich J.K., Gordon J.I., Huttley G.A., Kelley S.T.,
764 Knights D., Koenig J.E., Ley R.E., Lozupone C.A., McDonald D., Muegge B.D.,
765 Pirrung M., Reeder J., Sevinsky J.R., Turnbaugh P.J., Walters W.A., Widmann J.,
766 Yatsunenko T., Zaneveld J., & Knight R. (2010) QIIME allows analysis of high-
767 throughput community sequencing data Intensity normalization improves
768 color calling in SOLiD sequencing. *Nat. Methods*, **7**, 335–336.
769 Caporaso J.G., Lauber C.L., Walters W.A., Berg-lyons D., Lozupone C.A., Turnbaugh
770 P.J., Fierer N., & Knight R. (2011) Global patterns of 16S rRNA diversity at a

771 depth of millions of sequences per sample. *Proc. Natl. Acad. Sci.*, **108**, 4516–
772 4522.
773 Chen Y., Dumont M.G., Cébron A., & Murrell J.C. (2007) Identification of active
774 methanotrophs in a landfill cover soil through detection of expression of 16S
775 rRNA and functional genes. *Environ. Microbiol.*, **9**, 2855–69.
776 Cole J.R., Wang Q., Fish J.A., Chai B., McGarrell D.M., Sun Y., Brown C.T., Porras-Alfaro
777 A., Kuske C.R., & Tiedje J.M. (2014) Ribosomal Database Project: data and tools
778 for high throughput rRNA analysis. *Nucleic Acids Res.*, **42**, D633–D642.
779 Conrad R. (1999) Contribution of hydrogen to methane production and control of
780 hydrogen concentrations in methanogenic soils and sediments. *FEMS Microbiol.*
781 *Ecol.*, **28**, 193–202.
782 Delmas R.A., Tathy J.P., & Cros B. (1992a) Atmospheric methane budget in Africa. *J.*
783 *Atmos. Chem.*, **14**, 395–409.
784 Delmas R., Servant J., Tathy J., Cros B., & Labat M. (1992b) Sources and sinks of
785 methane and carbone dioxide exchanges in mountain forest in Equatorial
786 Africa. *J. Geophys. Res.*, **97**, 6169–6179.
787 Fadrosh D.W., Ma B., Gajer P., Sengamalay N., Ott S., Brotman R.M., & Ravel J. (2014)
788 An improved dual-indexing approach for multiplexed 16S rRNA gene
789 sequencing on the Illumina MiSeq platform. *Microbiome*, **2**, 1–7.
790 Freitag T.E. & Prosser J.I. (2009) Correlation of methane production and functional
791 gene transcriptional activity in a peat soil. *Appl. Environ. Microbiol.*, **75**, 6679–
792 87.
793 Freitag T.E., Toet S., Ineson P., & Prosser J.I. (2010) Links between methane flux and
794 transcriptional activities of methanogens and methane oxidizers in a blanket
795 peat bog. *FEMS Microbiol. Ecol.*, **73**, 157–165.
796 Garcia J.L., Patel B.K., & Ollivier B. (2000) Taxonomic, phylogenetic, and ecological
797 diversity of methanogenic Archaea. *Anaerobe*, **6**, 205–26.
798 Gavlak R., Horneck D., Miller R.O., & Kotuby-Amarcher J. (2003) Soil, Plant, and
799 Water Reference Methods for the Western Region. *West. Reg. Ext. Publ.*, **WREP-**
800 **125**, .
801 Graham E.B., Wieder W.R., Leff J.W., Weintraub S.R., Townsend A.R., Cleveland C.C.,
802 Philippot L., & Nemergut D.R. (2014) Do we need to understand microbial
803 communities to predict ecosystem function? A comparison of statistical
804 models of nitrogen cycling processes. *Soil Biol. Biochem.*, **68**, 279–282.
805 Ho A., Kerckhof F.-M., Luke C., Reim A., Krause S., Boon N., & Bodelier P.L.E. (2013)
806 Conceptualizing functional traits and ecological characteristics of methane-
807 oxidizing bacteria as life strategies. *Environ. Microbiol. Rep.*, **5**, 335–45.
808 Holmes A.J., Costello A., Lidstrom M.E., & Murrell J.C. (1995) Evidence that
809 particulate methane monooxygenase and ammonia monooxygenase may be
810 evolutionarily related. *FEMS Microbiol. Lett.*, **132**, 203–208.
811 Inkpen S.A., Douglas G.M., Brunet T.D.P., Leuschen K., Doolittle W.F., & Langille M.G.I.
812 (2017) The coupling of taxonomy and function in microbiomes. *Biol. Philos.*, .
813 Jones S.E. & Lennon J.T. (2010) Dormancy contributes to the maintenance of
814 microbial diversity. *Proc. Natl. Acad. Sci. U. S. A.*, **107**, 5881–6.
815 Kamke J., Taylor M.W., & Schmitt S. (2010) Activity profiles for marine sponge-
816 associated bacteria obtained by 16S rRNA vs 16S rRNA gene comparisons. *ISME*

J., **4**, 498–508.
Keller J. & Bridgham S. (2007) Pathways of anaerobic carbon cycling across an ombrotrophic-minerotrophic peatland gradient. *Limnol. Oceanogr.*, **52**, 96–107.
Kirschke S., Bousquet P., Ciais P., Saunois M., Canadell J.G., Dlugokencky E.J., Bergamaschi P., Bergmann D., Blake D.R., Bruhwiler L., Cameron-Smith P., Castaldi S., Chevallier F., Feng L., Fraser A., Heimann M., Hodson E.L., Houweling S., Josse B., Fraser P.J., Krummel P.B., Lamarque J.-F., Langenfelds R.L., Le Quere C., Naik V., O'Doherty S., Palmer P.I., Pison I., Plummer D., Poulter B., Prinn R.G., Rigby M., Ringeval B., Santini M., Schmidt M., Shindell D.T., Simpson I.J., Spahni R., Steele L.P., Strode S.A., Sudo K., Szopa S., van der Werf G.R., Voulgarakis A., van Weele M., Weiss R.F., Williams J.E., & Zeng G. (2013) Three decades of global methane sources and sinks. *Nat. Geosci.*, **6**, 813–823.
Knief C. (2015) Diversity and habitat preferences of cultivated and uncultivated aerobic methanotrophic bacteria evaluated based on pmoA as molecular marker. *Front. Microbiol.*, **6**, 1–38.
Kolb S. (2009) The quest for atmospheric methane oxidizers in forest soils. *Environ. Microbiol. Rep.*, **1**, 336–346.
Kozich J.J., Westcott S.L., Baxter N.T., Highlander S.K., & Schloss P.D. (2013) Development of a dual-index sequencing strategy and curation pipeline for analyzing amplicon sequence data on the MiSeq Illumina sequencing platform. *Appl. Environ. Microbiol.*, **79**, 5112–20.
Kulichevskaya I.S., Danilova O. V, Tereshina V.M., Kevbrin V. V, & Dedysh S.N. (2014) Descriptions of Roseiarcus fermentans gen. nov., sp. nov., a bacteriochlorophyll a-containing fermentative bacterium related phylogenetically to alphaproteobacterial methanotrophs, and of the family Roseiarcaceae fam. nov. *Int. J. Syst. Evol. Microbiol.*, **64**, 2558–2565.
Lee M.E., Alonso A., Dallmeier F., Campbell P., & Pauwels O.S.G. (2006) The Gamba Complex of Protected Areas: An Illustration of Gabon's Biodiversity. *Bull. Biol. Soc. Washingt.*, 229–242.
Legendre P. (1993) Spatial autocorrelation: trouble or new paradigm? *Ecology*, **74**, 1659–1673.
Lennon J.T. & Jones S.E. (2011) Microbial seed banks: the ecological and evolutionary implications of dormancy. *Nat. Rev. Microbiol.*, **9**, 119–30.
Loreau M., Naeem S., Inchausti P., Bengtsson J., Grime J.P., Hector A., Hooper D.U., Huston M.A., Raffaelli D., Schmid B., Tilman D., & Wardle D.A. (2001) Biodiversity and Ecosystem Functioning: Current Knowledge and Future Challenges. *Science (80-.).*, **294**, 804 LP-808.
Louca S., Polz M.F., Mazel F., Albright M.B.N., Huber J.A., Connor M.I.O., Ackermann M., Hahn A.S., Srivastava D.S., Crowe S.A., Doebeli M., & Parfrey L.W. (2018) Function and functional redundancy in microbial systems. *Nat. Ecol. Evol.*, .
Ma K., Conrad R., & Lu Y. (2012) Responses of methanogen mcrA genes and their transcripts to an alternate dry/wet cycle of paddy field soil. *Appl. Environ. Microbiol.*, **78**, 445–54.
MacDonald J.A., Jeeva D., Eggleton P., Davies R., Bignell D.E., Fowler D., Lawton J., & Maryati M. (1999) The effect of termite biomass and anthropogenic disturbance on the CH4 budgets of tropical forests in Cameroon and Borneo. *Glob. Chang.*

Biol., **5**, 869–879.
Martiny A.C., Treseder K., & Pusch G. (2013) Phylogenetic conservatism of functional traits in microorganisms. *ISME J.*, **7**, 830–8.
McCalley C.K., Woodcroft B.J., Hodgkins S.B., Wehr R. a., Kim E.-H., Mondav R., Crill P.M., Chanton J.P., Rich V.I., Tyson G.W., & Saleska S.R. (2014) Methane dynamics regulated by microbial community response to permafrost thaw. *Nature*, **514**, 478–481.
Megonigal J.P., Mines M.E., & Visscher P.T. (2004) Anaerobic Metabolism: Linkages to Trace Gases and Aerobic Processes. *Biogeochemistry* pp. 350–362. Gulf Professional Publishing,
Nazaries L., Murrell J.C., Millard P., Baggs L., & Singh B.K. (2013a) Methane, microbes and models: fundamental understanding of the soil methane cycle for future predictions. *Environ. Microbiol.*, **15**, 2395–417.
Nazaries L., Pan Y., Bodrossy L., Baggs E.M., Millard P., Murrell J.C., & Singh B.K. (2013b) Evidence of microbial regulation of biogeochemical cycles from a study on methane flux and land use change. *Appl. Environ. Microbiol.*, **79**, 4031–40.
Oksanen J., Blanchet F.G., Roeland K., Legendre P., Minchin P., O'Hara R.B., Simpson G., Solymos P., Stevens M.H.H., & Wagner H. (2015) vegan: Community ecology package. .
Papp K., Hungate B.A., & Schwartz E. (2018a) Microbial rRNA Synthesis and Growth Compared through Quantitative Stable Isotope Probing with H218O. *Appl. Environ. Microbiol.*, **84**, 1–11.
Papp K., Mau R.L., Hayer M., Koch B.J., Hungate B.A., & Schwartz E. (2018b) Quantitative stable isotope probing with H218O reveals that most bacterial taxa in soil synthesize new ribosomal RNA. *ISME J.*, 18–20.
R Core Team (2018) R: A language and environment for statistical computing. .
Ramakers C., Ruijter J.M., Deprez R.H.L., & Moorman A.F.. (2003) Assumption-free analysis of quantitative real-time polymerase chain reaction (PCR) data. *Neurosci. Lett.*, **339**, 62–66.
Rocca J.D., Hall E.K., Lennon J.T., Evans S.E., Waldrop M.P., Cotner J.B., Nemergut D.R., Graham E.B., & Wallenstein M.D. (2014) Relationships between protein-encoding gene abundance and corresponding process are commonly assumed yet rarely observed. *ISME J.*, **9**, 1693–1699.
Ross M.O. & Rosenzweig A.C. (2017) A tale of two methane monooxygenases. *J. Biol. Inorg. Chem.*, **22**, 307–319.
Ruijter J.M., Ramakers C., Hoogaars W.M.H., Karlen Y., Bakker O., van den Hoff M.J.B., & Moorman a F.M. (2009) Amplification efficiency: linking baseline and bias in the analysis of quantitative PCR data. *Nucleic Acids Res.*, **37**, e45.
Schimel J.P. (1995) Ecosystem Consequences of Microbial Diversity and Community Structure. *Arctic and Alpine Biodiversity: Patterns, Causes and Ecosystem Consequences* (ed. by F.S. Chapin III and C. Körner), pp. 239–254. Springer-Verlag, Berlin.
Schimel J.P. & Gulledge J. (1998) Microbial community structure and global trace gases. *Glob. Chang. Biol.*, **4**, 745–758.
Schmieder R. & Edwards R. (2011) Quality control and preprocessing of metagenomic datasets. *Bioinformatics*, **27**, 863–864.

Schnyder E., Bodelier P., Hartmann M., Henneberger R., & Niklaus P. (2018) Positive diversity-functioning relationships in model communities of methanotrophic bacteria. *Ecology*, **99**, 714–723.

Sierocinski P., Bayer F., Melia G.Y., Großkopf T., Alston M., Swarbreck D., Hobbs P.J., Soyer O.S., & Buckling A. (2018) Biodiversity – function relationships in methanogenic communities. *Mol. Ecol.*, **27**, 4641–4651.

Sierocinski P., Milferstedt K., Bayer F., Großkopf T., Alston M., Bastkowski S., Swarbreck D., Hobbs P.J., Soyer O.S., Hamelin J., & Buckling A. (2017) A Single Community Dominates Structure and Function of a Mixture of Multiple Methanogenic. *Curr. Biol.*, 3390–3395.

Sjögersten S., Black C.R., Evers S., Hoyos-Santillan J., Wright E.L., & Turner B. (2014) Tropical wetlands: A missing link in the global carbon cycle? *Global Biogeochem. Cycles*, **28**, 1371–1386.

Steinberg L.M. & Regan J.M. (2008) Phylogenetic comparison of the methanogenic communities from an acidic, oligotrophic fen and an anaerobic digester treating municipal wastewater sludge. *Appl. Environ. Microbiol.*, **74**, 6663–71.

Tathy J.P., Cros B., Delmas R.A., Marenco A., Servant J., & Labat M. (1992) Methane emission from flooded forest in central Africa. *J. Geophys. Res. Atmos.*, **97**, 6159–6168.

Tilman D. & Downing J.A. (1994) Biodiversity and stability in grasslands. *Nature*, **367**, 363–365.

Tilman D., Wedin D., & Knops J. (1996) Productivity and sustainability influenced by biodiversity in grassland ecosystems. *Nature*, **379**, 718.

Wang Q., Garrity G.M., Tiedje J.M., & Cole J.R. (2007) Naive Bayesian Classifier for Rapid Assignment of rRNA Sequences into the New Bacterial Taxonomy. *Appl. Environ. Microbiol.*, **73**, 5261–5267.

White F. (1979) The Guineo-Congolian Region and Its Relationships to Other Phytochoria. *Bull. du Jard. Bot. Natl. Belgique / Bull. van Natl. Plantentuin van Belgie*, **49**, 11–55.

Wickham H. (2009) *ggplot2: elegant graphics for data analysis.* Springer Science & Business Media,

Zhang J., Kobert K., Flouri T., & Stamatakis A. (2014) PEAR: a fast and accurate Illumina Paired-End reAd mergeR. *Bioinformatics*, **30**, 614–620.